Inorganic Chemistry

Article

pubs.acs.org/IC

Mono-, Bi-, and Trinuclear Bis-Hydrated Mn^{2+} Complexes as Potential MRI Contrast Agents

Attila Forgács,[†] Martín Regueiro-Figueroa,[‡] José Luis Barriada,[§] David Esteban-Gómez,[‡] Andrés de Blas,[‡] Teresa Rodríguez-Blas,[‡] Mauro Botta,*[,†] and Carlos Platas-Iglesias*[,‡]

[†]Dipartimento di Scienze e Innovazione Tecnologica, Università del Piemonte Orientale "A. Avogadro", Viale T. Michel 11, 15121 Alessandria, Italy

[‡]Grupo QUICOOR, Centro de Investigaciones Científicas Avanzadas (CICA) and Departamento de Química Fundamental and [§]Departamento de Química Física e Enxeñaría Química I, Universidade da Coruña, Campus da Zapateira, Rúa da Fraga 10, 15008 A Coruña, Spain

Supporting Information

ABSTRACT: We report a series of ligands containing pentadentate 6,6′-((methylazanediyl)bis(methylene))dipicolinic acid binding units that form mono- (H_2dpama), di- (mX(H_2dpama)$_2$), and trinuclear (mX(H_2dpama)$_3$) complexes with Mn^{2+} containing two coordinated water molecules per metal ion, which results in pentagonal bipyramidal coordination around the metal ions. In contrast, the hexadentate ligand 6,6′-((ethane-1,2-diylbis-(azanediyl))bis(methylene))dipicolinic acid (H_2bcpe) forms a complex with distorted octahedral coordination around Mn^{2+} that lacks coordinated water molecules. The protonation constants of the ligands and the stability constants of the Mn^{2+}, Cu^{2+}, and Zn^{2+} complexes were determined using potentiometric and spectrophotometric titrations in 0.15 M NaCl. The pentadentate dpama^{2-} ligand and the di- and trinucleating mX(dpama)$_2^{4-}$ and mX(dpama)$_3^{6-}$ ligands provide metal complexes with stabilities that are very similar to that of the complex with the hexadentate ligand bcpe^{2-}, with log β_{101} values in the range 10.1−11.6. Cyclic voltammetry experiments on aqueous solutions of the [Mn(bcpe)] complex reveal a quasireversible system with a half-wave potential of +595 mV versus Ag/AgCl. However, [Mn(dpama)] did not suffer oxidation in the range 0.0−1.0 V, revealing a higher resistance toward oxidation. A detailed ^{1}H NMRD and ^{17}O NMR study provided insight into the parameters that govern the relaxivity for these systems. The exchange rate of the coordinated water molecules in [Mn(dpama)] is relatively fast, k_{ex}^{298} = (3.06 ± 0.16) × 10^8 s^{-1}. The trinuclear [mX(Mn(dpama)$(H_2O)_2)_3$] complex was found to bind human serum albumin with an association constant of 1286 ± 55 M^{-1} and a relaxivity of the adduct of 45.2 ± 0.6 mM^{-1} s^{-1} at 310 K and 20 MHz.

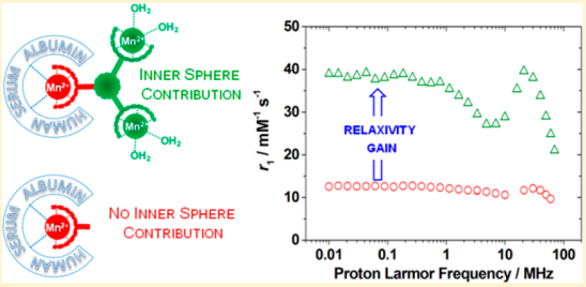

INTRODUCTION

Magnetic resonance imaging (MRI) is an important tool in medical diagnosis that provides high-quality images of soft tissues with very high spatial resolution. The introduction of some Gd^{3+} complexes as contrast agents (CAs) in MRI has stimulated thriving investigation activities on the coordination chemistry of this metal ion and other lanthanide ions.[1] Commercially available Gd^{3+}-based CAs are complexes with polyamino/polycarboxylate octadentate ligands that leave vacant a coordination position for a water molecule.[2] The coordinated water molecule is involved in a fast exchange with the water of the surrounded tissues, which imparts an efficient mechanism for the increase of the relaxation rates of proton nuclei of water molecules. The Gd^{3+} ion was selected for the preparation of CAs owing to its high effective magnetic moment and relatively slow electron spin relaxation, which is related to its symmetrical ^{8}S electronic ground state. However, high-spin Mn^{2+} and Fe^{3+} complexes with d^5 configuration also present relatively slow electron spin relaxation and rather high effective magnetic moments, and thus stable complexes of these metal ions might find application as MRI CAs, replacing the traditional Gd^{3+}-based compounds.[3−5]

The application of Mn^{2+} complexes as MRI CAs was already envisaged in the early times of MRI in the late 1980s.[6,7] As a result of these pioneering studies, a Mn^{2+}-based CA, mangafodipir trisodium (Mndpdp, TESLASCAN, Chart 1), was approved for clinical use. More recently, a mixture of $MnCl_2$, alanine, and vitamin D_3, denoted as CMC-001, has been proposed as a CA for visualization of liver and bile, and it is currently undergoing phase III clinical trials.[8] Furthermore, preclinical safety assessment of Mndpdp serendipitously revealed superoxide dismutase activity, a useful property that can be potentially exploited for the treatment of several pathological conditions characterized by oxidative stress (i.e., cancer treatment, acute myocardial infarction, etc.).[9] An important advantage of Mn^{2+} CAs over the traditional Gd^{3+} counterparts is the lower toxicity of free Mn^{2+}, which is

Received: July 24, 2015
Published: September 23, 2015

DOI: 10.1021/acs.inorgchem.5b01677
Inorg. Chem. 2015, 54, 9576−9587

Chart 1. Chemical Structure of the Ligands Discussed in This Work

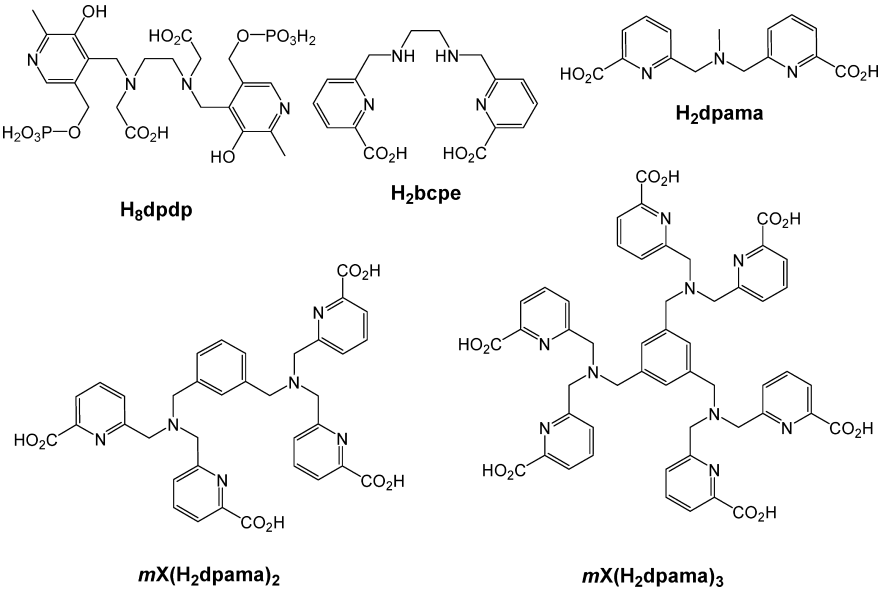

Scheme 1. Synthesis of mX$(H_2$dpama$)_3$

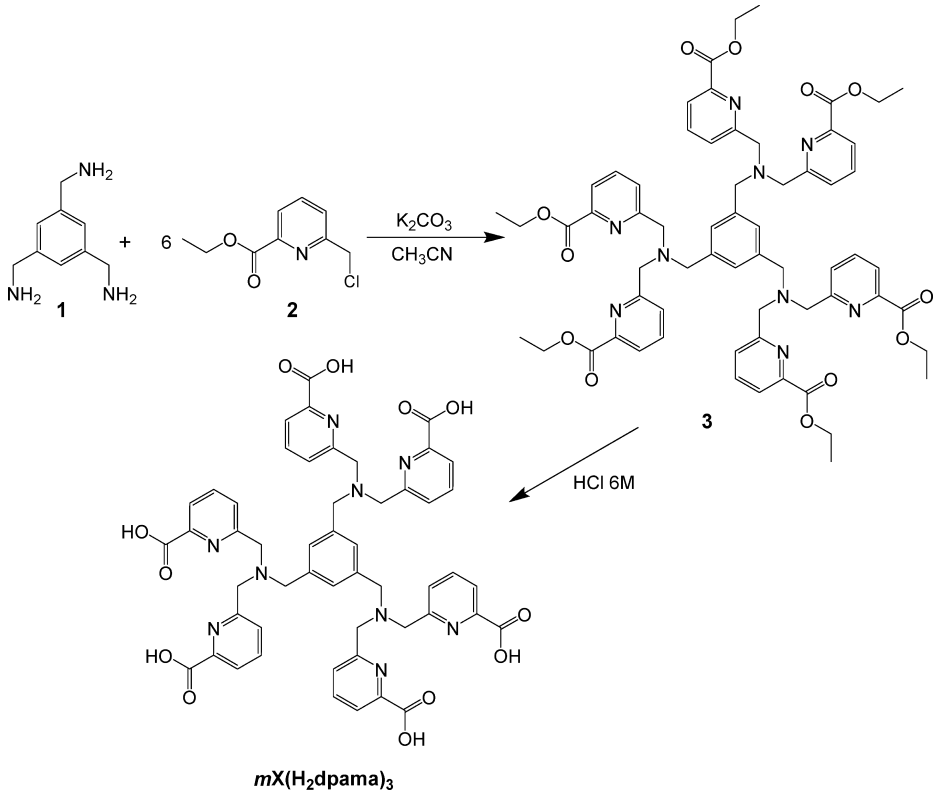

highlighted by the formulation of CMC-001. On the other hand, the lower number of unpaired electrons of Mn^{2+} complexes with respect to Gd^{3+} analogues generally results in lower relaxivities of the Mn^{2+} complexes at high fields (>20 MHz).[10] Relaxivity, r_{1p}, is defined as the relaxation enhancement of water protons promoted by the paramagnetic agent at 1 mM concentration, and it is a measure of the efficiency of the CA in vitro. An obvious strategy to increase relaxivity is to increase the number of water molecules coordinated to the paramagnetic ion (q), as the inner-sphere contribution to relaxivity is directly proportional to q. This approach has been successfully used to increase the relaxivities of Gd^{3+} complexes, although generally reducing the denticity of the ligand to increase the hydration number results in lower thermodynamic stabilities of the complexes.[11] Some attempts have also been made to obtain bis-hydrated Mn^{2+} complexes as potential MRI contrast agents, but the expected relaxivity gain was not observed due to a low exchange rate of the coordinated water molecule with the bulk water.[12] A second advantage of Mn-based contrast agents is that they can be used as redox-sensitive MRI probes, providing that a suitable ligand stabilizes both Mn^{2+} and Mn^{3+}.[13−15]

DOI: 10.1021/acs.inorgchem.5b01677
Inorg. Chem. 2015, 54, 9576−9587

In a recent communication,[16] we reported ligands H_2dpama and mX(H_2dpama)$_2$ (Chart 1), which were shown to form mono- and binuclear Mn^{2+} complexes containing two water molecules coordinated to each metal center. These complexes displayed remarkably high relaxivities, as well as relatively high affinities toward human serum albumin (HSA). Herein, we report the trinucleating ligand mX(H_2dpama)$_3$ and a detailed relaxometric characterization of the Mn^{2+} complexes with the three ligands using ^{1}H relaxometry and ^{17}O NMR measurements. Furthermore, the ligand protonation constants and stability constants of the metal complexes were determined using potentiometric measurements. Cyclic voltammetry experiments were also carried out to investigate the relative stability of the Mn^{2+} and Mn^{3+} complexes. In another work,[17] we have reported the hexadentate ligand H_2bcpe, which was shown to form rather stable complexes with different divalent and trivalent metal ions.[18,19] Given the ability of Mn^{2+} complexes to form both six- and seven-coordinate complexes in aqueous solution, we have also checked whether the [Mn(bcpe)] complex contains a coordinated water molecule or not by using ^{1}H relaxometric measurements and X-ray diffraction studies.

RESULTS AND DISCUSSION

Syntheses and Characterization. The syntheses of ligands H_2dpama and mX(H_2dpama)$_2$ and their Mn^{2+} complexes were reported in a preliminary communication.[16] The synthesis of mX(H_2dpama)$_3$ (Scheme 1) was achieved in two steps by reaction of benzene-1,3,5-triyltrimethanamine (**1**) and 6-chloromethylpyridine-2-carboxylic acid ethyl esther (**2**) in the presence of K_2CO_3 and subsequent hydrolysis of the ethyl ester groups in 6 M HCl. Reaction of the ligand with $MnCl_2\cdot4H_2O$ in the presence of trimethylamine produced the desired charge-neutral complex. The high-resolution mass spectrum of the complex (ESI^+) shows an intense peak due to the [Na_2mX(Mndpama)$_3$]$^{2+}$ entity. The excellent agreement between the experimental and calculated isotopic distribution patterns confirms the formation of the trinuclear complex (Figure S3, Supporting Information).

The relaxometric studies reported in our previous work have shown that the [Mn(dpama)] complex contains two water molecules coordinated to Mn^{2+}. Herein, DFT calculations (TPSSh/SVP level) were conducted in order to assess whether the coordination of three Mn^{2+} ions by the mX(H_2dpama)$_3$ ligand is sterically feasible (Figure 1). Following our previous studies, two second-sphere water molecules have been explicitly included in our model to improve the values of the calculated Mn−O_{water} distances.[20] According to our calculations the three metal centers describe a nearly equilateral triangle with Mn···Mn distances of 10.4−11.1 Å. The average bond distances of the metal coordination environment are very similar to those reported in our previous communication for the complex of $dpama^{2-}$ using the same methodology.[16] The calculated bond distances of the metal coordination environment are also in very good agreement with those observed in the solid state for a dinuclear Mn^{2+} complex containing two $dpama^{2-}$ units linked by an ethyl group.[21] Each of the three Mn^{2+} ions presents distorted pentagonal bipyramidal coordination, where the five donor atoms of each $dpama^{2-}$ unit occupy the equatorial positions, and two water molecules coordinate apically and complete the inner sphere of the metal ion.

The synthesis of H_2bcpe was achieved by following the previously reported procedure.[17] Reaction of H_2bcpe with

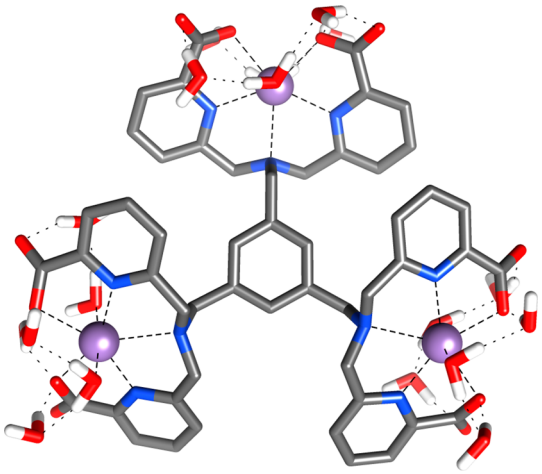

Figure 1. Optimized geometry of the [mX(Mn(dpama)$(H_2O)_2)_3$]·$12H_2O$ complex obtained with DFT calculations performed in aqueous solution at the TPSSh/SVP level. Average bond distances (Å) of the Mn^{2+} coordination environment: Mn−O_{water} 2.213(19); Mn−O_{COO} 2.315(58); Mn−N_{amine} 2.620(6); Mn−N_{PY} 2.280(14). Hydrogen atoms, except those of water molecules, have been omitted for simplicity.

$Mn(ClO_4)_2\cdot6H_2O$ in the presence of trimethylamine provided the charge-neutral [Mn(bcpe)] complex, which was isolated in 60% yield. The high-resolution mass spectrum of the complex (ESI^+) shows an intense peak attributable to the [Mn(Hbcpe)]$^+$ entity, which confirms the formation of the complex (Figure S4, Supporting Information). Slow evaporation of a solution of the complex in water provided single crystals of formula [Mn(bcpe)]·$2H_2O$ suitable for X-ray diffraction analyses. Crystals contain the expected neutral complex and noncoordinated water molecules hydrogen bonded to the oxygen atoms of the carboxylate groups. Figure 2 shows a view

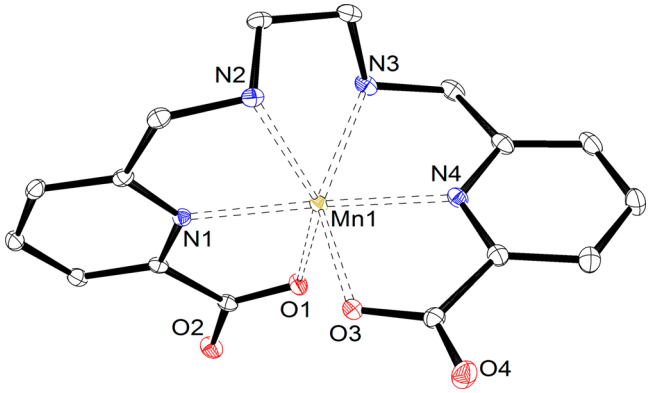

Figure 2. View of the X-ray structure of the [Mn(bcpe)] complex. Water molecules and hydrogen atoms are omitted for simplicity. The ORTEP plot is at the 30% probability level. Bond distances (Å): Mn(1)−O(1), 2.1771(12); Mn(1)−O(3), 2.1783(12); Mn(1)−N(1), 2.1919(15); Mn(1)−N(4), 2.1948(15); Mn(1)−N(2), 2.3046(14); Mn(1)−N(3), 2.3217(14).

of the structure of the complex and bond distances of the metal coordination environment. The metal ion is directly coordinated to six donor atoms of the ligand, as observed previously for the Zn^{2+},[17] Cd^{2+},[17] Ga^{3+},[18] and Cu^{2+} [19] complexes. The two aminopicolinate units bind meridionally through their N-amine, N-pyridine, and O-carbonyl donor atoms. The metal

DOI: 10.1021/acs.inorgchem.5b01677
Inorg. Chem. 2015, 54, 9576−9587

coordination environment can be described as distorted octahedral, with the *trans* angle N1−Mn1−N4 being relatively close to the ideal value of 180° [176.22(5)°]. However, the *trans* angles O(1)−Mn(1)−N(2) [143.24(5)°] and O(3)−Mn(1)−N(3) [144.32(5)°] show large deviations from the ideal value for a regular octahedron, pointing to a large amount of distortion of the octahedral coordination.

Ligands stabilizing both Mn^{2+} and Mn^{3+} can be of potential use in the preparation of redox-activated MRI contrast agents.[13,14] Thus, the relative stability of the Mn^{2+} and Mn^{3+} complexes of $bcpe^{2-}$ and $dpama^{2-}$ was assessed by using cyclic voltammetry experiments in aqueous solutions (NaCl 0.15 M, pH = 7.0). The cyclovoltammetric curve obtained for [Mn(bcpe)] (Figure 3) is characteristic of a quasireversible

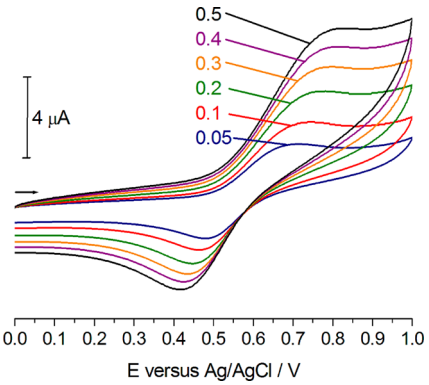

Figure 3. Cyclovoltammograms recorded for a ca. 2 mM aqueous solution of [Mn(bcpe)] (0.15 M NaCl, pH 7.0) at varying scan rates from 0.05 to 0.5 V/s.

system with a half-wave potential of +595 mV (ΔE_p = 230 mV) versus Ag/AgCl. The electrochemical process is controlled by diffusion, as the anodic and cathodic current intensities vary linearly with the square root of the scan rate in the range 50−500 mV s^{-1} (Figure S5, Supporting Information). The half-wave potential observed for [Mn(bcpe)] reveals that the $bcpe^{2-}$ ligand stabilizes divalent Mn to a higher extent than $edta^{4-}$, for which a half-cell potential of +633 mV has been reported versus *nhe*,[13a] which corresponds to +423 mV versus Ag/AgCl in 3 M KCl.[22] Cyclic voltammetry experiments carried out in solutions of [Mn(dpama)] did not show any oxidation in the range 0.0−1.0 V (versus Ag/AgCl), revealing a higher resistance toward oxidation, which is likely related to the pentagonal bipyramidal coordination geometry around the metal ion. Indeed, experience with simple inorganic complexes suggests that five- and seven-coordinate Mn^{2+} complexes are more difficult to oxidize to Mn^{3+} than octahedral complexes.[23]

Ligand Protonation Constants and Stability Constants of the Metal Complexes. The protonation constants ($\log K_i^H$) of the four ligands investigated in this work have been determined by pH-potentiometry in 0.15 M NaCl. The values of the constants and standard deviations are reported in Table 1. The protonation constants are defined by eq 1:

$$H_{i-1}L + H^+ \rightleftharpoons H_iL$$

$$K_i^H = \frac{[H_iL]}{[H_{i-1}L][H^+]} \quad i = 1, 2, ..., 8 \tag{1}$$

By taking into account the protonation constants and protonation scheme of picolinic acid,[24] it can be assumed that the first and second protonation constants of $dpama^{2-}$ correspond to the amine nitrogen and the carboxyl groups of the picolinate fragments, respectively. The first and second protonation constants of $mX(dpama)_2^{4-}$ are related to the protonation of the amine nitrogen atoms, whereas subsequent protonations of the ligand take place at the carboxylate groups. Similarly, the $\log K_1^H$, $\log K_2^H$, and $\log K_3^H$ values of $mX(dpama)_3^{6-}$ are also attributed to the protonation of the amine nitrogen atoms, while subsequent protonation processes take place at the carboxylate groups of the picolinate residues.

The difference between successive protonation constants of identical and independent coordination sites is expected to follow the statistical factor,[25] which predicts a difference between two successive identical protonation sites of $\Delta\log K^H = \log K_1^H - \log K_2^H = 0.6$. In the case of three independent protonation sites this factor reduces to $\Delta\log K^H = 0.5$. The second protonation constant of $mX(dpama)_2^{4-}$ is ca. 1.3 log K units lower than $\log K_1^H$. This difference is larger than that expected for the statistical factor, which is explained by the repulsive electrostatic interaction between the protonated amine nitrogen atoms in the bis-protonated species. Similarly to the $mX(dpama)_2^{4-}$ ligand, the differences between $\log K_1^H$, $\log K_2^H$ and $\log K_3^H$ of $mX(dpama)_3^{6-}$ are larger than expected according to the statistical factor. However, the protonation of the carboxylate groups of $mX(dpama)_2^{4-}$ characterized by $\Delta\log K^H = \log K_3^H - \log K_4^H = 0.8$, as well as those of $mX(dpama)_3^{6-}$ given by $\Delta\log K^H = \log K_4^H - \log K_5^H = 0.6$, approaches the behavior expected according to the statistical factor. This is likely related to the longer distances between the involved protonation sites in comparison to the amine nitrogen

Table 1. Protonation Constants of Ligands $bcpe^{2-}$, $dpama^{2-}$, $mX(dpama)_2^{4-}$, $mX(dpama)_3^{6-}$, and Picolinate (0.15 M NaCl, 298 K)

	$dpama^{2-}$	$mX(dpama)_2^{4-}$	$mX(dpama)_3^{6-}$	$bcpe^{2-}$	picolinate[a]
$\log K_1^H$	7.82(1)	7.77(1)	7.73(1)	8.83(2)	5.25
$\log K_2^H$	3.71(2)	6.49(1)	6.82(1)	6.22(3)	0.92
$\log K_3^H$	2.61(2)	4.24(2)	6.06(1)	3.27(3)	
$\log K_4^H$		3.45(2)	4.31(1)	2.03(3)	
$\log K_5^H$		2.93(2)	3.70(1)		
$\log K_6^H$		2.24(2)	3.30(1)		
$\log K_7^H$			2.79(1)		
$\log K_8^H$			2.36(1)		
$\log K_9^H$			1.01(3)		
$\sum\log K_i^H$	14.14	27.13	38.09	20.36	6.17

[a]Taken from ref 24.

DOI: 10.1021/acs.inorgchem.5b01677
Inorg. Chem. 2015, 54, 9576−9587

Table 2. Stability and Protonation Constants of Mn^{2+} Complexes Formed with $bcpe^{2-}$, $dpama^{2-}$, $mX(dpama)_2^{4-}$, and $mX(dpama)_3^{6-}$ Ligands (0.15 M NaCl and 298 K)

	$bcpe^{2-}$	$dpama^{2-}$	$mX(dpama)_2^{4-}$	$mX(dpama)_3^{6-}$
log K(ML)	10.63(2)	10.13(2)	11.60(6)	10.99(9)
log K(MHL)	3.42(7)	2.57(4)	6.50(4)	7.23(9)
log K(MH_2L)			3.61(2)	6.11(7)
log K(MH_3L)			2.56(1)	4.07(6)
log K(MH_4L)				3.29(3)
log K(MH_5L)				2.73(4)
log K(Mn_2L)			8.43(2)	9.17(9)
log K(Mn_2LH)				6.00(9)
log K(Mn_3L)				8.51(4)
log K(Mn_3LH)				2.54(3)
log K($MnLH_{-1}$)		11.09(4)	10.41(8)	

Table 3. Stability and Protonation Constants of Zn^{2+} and Cu^{2+} Complexes Formed with the $bcpe^{2-}$ and $dpama^{2-}$ Ligands (0.15 M NaCl, 298 K)

	Zn^{2+}:$dpama^{2-}$	Cu^{2+}:$dpama^{2-}$	Zn^{2+}:$bcpe^{2-}$	Cu^{2+}:$bcpe^{2-}$
log β_{101}(ML)	11.75(1)	13.32(4)[a]	17.53(2)	19.846(9)[a]
log K_{111}(MHL)	1.51(2)	3.60(4)	2.07(2)	1.45(3)
log K_{121}(MH_2L)		1.40(4)		
log K_{1-11}($MH_{-1}L$)	9.18(6)	9.53(4)		
log K_{1-21}($MH_{-2}L$)	11.16(7)	11.60(6)		

[a]Determined by spectrophotometry.

atoms. Comparison of the $\sum\log K_i^H$ of $dpama^{2-}$ (14.14), $\sum\log K_i^H/2$ of ditopic $mX(dpama)_2^{4-}$ (13.56), and $\sum\log K_i^H/3$ of tritopic $mX(dpama)_3^{6-}$ (12.36) indicates that the total basicity of $dpama^{2-}$ is higher than that of the average basicity of the $dpama^{2-}$ units in $mX(dpama)_2^{4-}$ and $mX(dpama)_3^{6-}$.

The protonation constants determined for $bcpe^{2-}$ in 0.15 M NaCl are very similar to those determined previously using a 0.1 M $(Me_4N)(NO_3)$ ionic strength,[17] which points to a weak coordination of the ligand to Na^+. The first and second protonation processes occur at the amine nitrogen atoms of the ligand, while the third and fourth protonation constants are assigned to the protonation of the carboxylate groups of the picolinate moieties.

The stability and protonation constants of the Mn^{2+} complexes formed with $bcpe^{2-}$, $dpama^{2-}$, $mX(dpama)_2^{4-}$, and $mX(dpama)_3^{6-}$ ligands were determined by pH-potentiometric titration. Furthermore, we have also determined the stability and protonation constants of the Zn^{2+} and Cu^{2+} complexes with $dpama^{2-}$. The metal-to-ligand concentration ratios were 1:1, as well as 2:1 and 3:1 in the case of $mX(dpama)_2^{4-}$ and $mX(dpama)_3^{6-}$. The stability and protonation constants of the metal complexes are defined by eqs 2−5:

$$M + L \rightleftharpoons ML$$

$$K_{ML} = \frac{[ML]}{[M][L]} \quad (2)$$

$$MH_{i-1}L + H^+ \rightleftharpoons MH_iL$$

$$K_{MH_iL} = \frac{[MH_iL]}{[MH_{i-1}L][H^+]} \quad i = 1-5 \quad (3)$$

$$M_{i-1}L + M \rightleftharpoons M_iL$$

$$K_{M_iL} = \frac{[M_iL]}{[M_{i-1}L][M]} \quad i = 2, 3 \quad (4)$$

$$M_iL + H^+ \rightleftharpoons M_iLH$$

$$K_{M_iLH} = \frac{[M_iLH]}{[M_iL][H^+]} \quad i = 2, 3 \quad (5)$$

The stability constants and protonation constants of the metal complexes are reported in Tables 2 and 3. The log K(ML) values determined for the four Mn^{2+} complexes are quite similar, which shows that the pentadentate $dpama^{2-}$ ligand and the di- and trinucleating $mX(dpama)_2^{4-}$ and $mX(dpama)_3^{6-}$ ligands provide metal complexes with stabilities that are very similar to that of the complex with the hexadentate ligand $bcpe^{2-}$, with log K(ML) values in the range 10.1−11.6.

The stability of the Mn^{2+} complex of the pentadentate ligand $dpama^{2-}$ is very similar to that of the complex with the hexadentate ligand $bcpe^{2-}$. The stability constants of the mononuclear Mn(dpama), $mX(Mndpama)_2$, and $mX(Mndpama)_3$ complexes are comparable, indicating that in all cases the Mn^{2+} ion is coordinated by a $dpama^{2-}$ unit characterized by similar metal ion affinity. Since the mononuclear $mXMn(dpama)_2$ and $mXMn(dpama)_3$ complexes have one and two noncoordinated $dpama^{2-}$ units, the free donor atoms can be protonated with the formation of several protonated MnH_iL species ($mX(dpama)_2$: i = 1−3; $mX(dpama)_3$: i = 1−5). The protonation constants of mononuclear $mXMn(dpama)_2$ and $mXMn(dpama)_3$ complexes (Table 2) are comparable to the corresponding log K_i^H values of the free ligands (Table 1).

The stability constants of the dinuclear ($mXMn_2(dpama)_2$, $mXMn_2(dpama)_3$) and trinuclear ($mXMn_3(dpama)_3$) complexes are very similar and somewhat lower than the log K(ML) values of the mononuclear $mXMn(dpama)_2$ and $mXMn(dpama)_3$ entities (Table 2). A recent study has reported virtually identical stability constants for the mono- and binuclear Mn^{2+} complexes of ditopic do3a-based ligands containing a long spacer separating the two metal binding

DOI: 10.1021/acs.inorgchem.5b01677
Inorg. Chem. 2015, 54, 9576−9587

units.[26] Thus, the slightly lower stability constants of the dinuclear and trinuclear Mn^{2+} complexes of mX(dpama)$_2$ and mX(dpama)$_3$ might be explained by the electron-withdrawing effect caused by the coordination of Mn^{2+} to a dpama^{2-} unit on the noncoordinated amine nitrogen atom of the neighbor dpama^{2-} moiety. Comparison of the log K(ML) value of Mn(dpama) (10.13) with the log K(M$_2$L)/2 value of dinuclear mXMn$_2$(dpama)$_2$ (10.01) and log K(M$_3$L)/3 value of trinuclear Mn$_3$(mX(dpama)$_3$) (9.56) indicates that the average Mn^{2+} affinities of the dpama^{2-} units in the mono-, bi-, and tritopic ligands decrease in the following order: dpama^{2-} > mX-(dpama)$_2^{4-}$ > mX(dpama)$_3^{6-}$.

The stabilities of the Mn^{2+}, Cu^{2+}, and Zn^{2+} complexes with a given ligand follow the order Mn^{2+} < Cu^{2+} > Zn^{2+}, in agreement with the Irving−Williams order.[27] The stability of the [Cu(bcpe)] complex is 9 orders of magnitude higher than that of [Mn(bcpe)], while the Zn^{2+} complex is about 7 orders of magnitude more stable than the Mn^{2+} one. In the case of the dpama^{2-} complexes the stabilities of the Zn^{2+} and Cu^{2+} complexes are only 1.6 and 3.2 log K units higher than that of the Mn^{2+} analogue. These results show that the pentadentate dpama^{2-} ligand is particularly well preorganized to provide a seven-coordinate Mn^{2+} complex with pentagonal bipyramidal coordination. Pentagonal bipyramidal coordination is far less favorable for Cu^{2+} and Zn^{2+} complexes,[28] which likely results in a modest increase of complex stability of the latter complexes with respect to Mn^{2+}.

The species distribution of the Mn^{2+}−dpama, Mn^{2+}−mX(dpama)$_2$, and Mn^{2+}−mX(dpama)$_3$ systems have been calculated by taking into account the equilibrium constants of Tables 1 and 2 (Figure 4; see also Figures S6−S8, Supporting Information). The dissociation of [Mn(dpama)] occurs below pH ∼5, while it represents the major species in solution up to pH ∼11. However, at pH > 8.5 deprotonation of the complex takes place with the formation of a MnH$_{-1}$L species, likely as a result of the coordination of a OH^- anion to the Mn^{2+} ion. The [mXMn$_2$(dpama)$_2$] and [mXMn$_3$(dpama)$_3$] complexes dissociate below pH ∼4, which results in the formation of complex species with reduced nuclearity. No evidence for the formation of hydroxo complexes was found in any of these cases.

Relaxometric Studies. The efficiency of a paramagnetic complex as a CA in vitro is often and conveniently assessed by its proton relaxivity, r_{1p}. The r_{1p} values determined for [Mn(bcpe)] and [Mn(dpama)] in the pH range ∼10.0−5.0 (20 MHz, 25 °C) are fairly constant (Figure S9, Supporting Information), while below pH 5.0 relaxivity progressively increases due to the dissociation of the complex and formation of $[Mn(H_2O)_6]^{2+}$,[29] in agreement with the speciation diagrams obtained from equilibrium data. The relaxivity measured for [Mn(bcpe)] is rather low (1.4 mM^{-1} s^{-1} at 25 °C, 20 MHz, pH 7.47) and compares well to those measured for [Mn(do3a)]$^-$, [Mn(dtpa)]$^{3-}$, and [Mn(1,7-do2a)], which lack inner-sphere water molecules (1.3−1.5 mM^{-1} s^{-1} at 25 °C and 20 MHz).[30] Thus, the relaxivity observed for [Mn(bcpe)] can be attributed to the outer-sphere mechanism, in full agreement with the X-ray structure of the complex described above. The relaxivity of [Mn(dpama)] is however clearly higher than the values measured for [Mn(bcpe)] and [Mn(edta)]$^{2-}$, the latter being a representative example of a Mn^{2+} complex containing one inner-sphere water molecule (Table 4).[30] This points to the presence of two coordinated water molecules in the [Mn-(dpama)] complex, as already anticipated in a preliminary communication.[16]

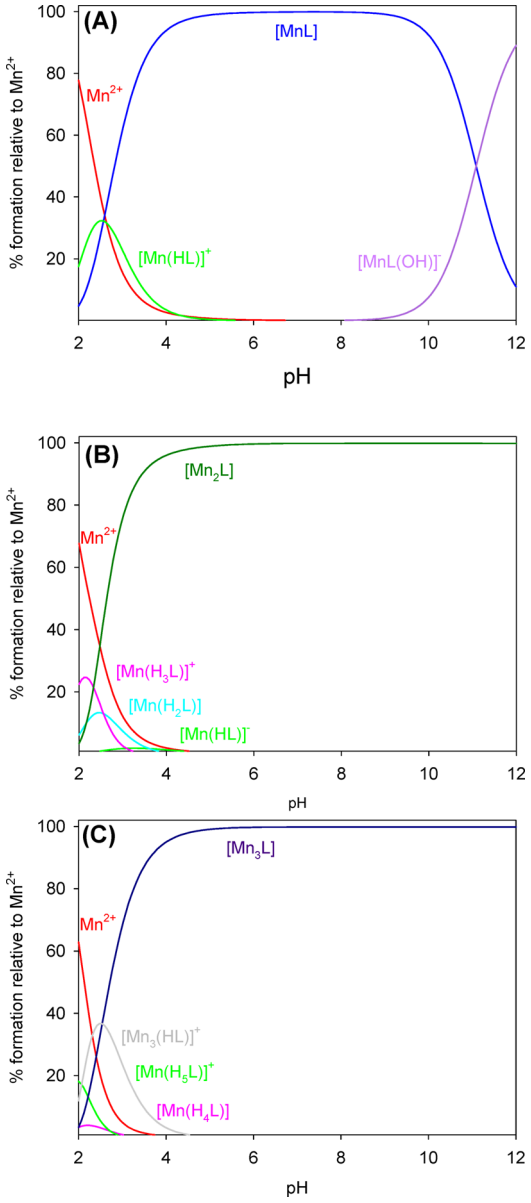

Figure 4. Species distribution diagrams of the Mn^{2+}−dpama ([Mn^{2+}] = [dpama] = 1.0 mM) (A), Mn^{2+}−mX(dpama)$_2$ ([Mn^{2+}] = 2 mM, [mX(dpama)$_2$] = 1.0 mM) (B), and Mn^{2+}−mX(dpama)$_3$ ([Mn^{2+}] = 3 mM, [mX(dpama)$_2$] = 1.0 mM) (C) systems (0.15 M NaCl, 298 K).

To gain more insight into the physicochemical parameters that govern the relaxivities observed for [Mn(bcpe)] and [Mn(dpama)], we recorded ^{1}H nuclear magnetic relaxation dispersion (^{1}H NMRD) profiles of aqueous solutions of these complexes in the proton Larmor frequency range 0.01−70 MHz, corresponding to magnetic field strengths varying between 2.343 × 10^{-4} and 1.645 T (Figure 5). The relaxivity of [Mn(dpama)] decreases with increasing temperature, a behavior typical of small chelates in which fast rotation of the complex in solution limits proton relaxivity. Furthermore, the ^{1}H NMRD profiles of [Mn(dpama)] show a single dispersion between 1 and 10 MHz, which rules out any scalar contribution to ^{1}H relaxivity.[29,31] Since the inner-sphere contribution to relaxivity depends upon a relatively large number of parameters, we have also recorded reduced transverse ^{17}O NMR relaxation rates and chemical shifts of an aqueous solution of [Mn-(dpama)] (3.89 mM, pH = 7.2). These data provide

DOI: 10.1021/acs.inorgchem.5b01677
Inorg. Chem. 2015, 54, 9576−9587

Table 4. Parameters Obtained from the Simultaneous Analysis of ^{17}O NMR and ^{1}H NMRD Data

	bcpe^{2-}	dpama^{2-}	mX(dpama)$_2^{4-}$	mX(dpama)$_3^{6-}$	edta^{4-}[b]
r_{1p} at 25/37 °C/mM^{-1} s^{-1}	1.4/1.2	5.3/4.2	8.6/6.1	11.4/8.3	3.3/2.8
$k_{ex}^{298}/10^8$ s^{-1}		3.06 ± 0.16	3.06[a]	3.06[a]	4.71
$\Delta H^{\ddagger}$/kJ mol^{-1}		28.1 ± 2.2	28.1[a]	28.1[a]	33.5
τ_R^{298}/ps		47.8 ± 0.9	95.8 ± 1.8	136 ± 3.0	57
E_r/kJ mol^{-1}		25.3 ± 0.6	27.3 ± 0.7	31.6 ± 1.0	21.8
τ_v^{298}/ps	19.9 ± 0.9	39.2 ± 5.6	57.6 ± 7.0	27.7 ± 3.4	27.9
E_v/kJ mol^{-1}	3.7 ± 0.7	1.0[a]	1.0[a]	1.0[a]	1.0[a]
$D_{MnH}^{298}/10^{-10}$ m^2 s^{-1}	21.8 ± 0.2	22.4[a]	22.4[a]	22.4[a]	23.1
E_{DMnH}/kJ mol^{-1}	21.6 ± 0.2	17.3[a]	17.3[a]	17.3[a]	18.9
$\Delta^2/10^{19}$ s^{-2}	9.0 ± 0.5	2.38 ± 0.39	1.48 ± 0.25	3.26 ± 0.50	6.9
$A_O/\hbar/10^6$ rad s^{-1}		−45.8 ± 0.8			−40.5
r_{MnH}/Å		2.74[a]	2.74[a]	2.74[a]	2.83[a]
a_{MnH}/Å	3.6[a]	3.6[a]	3.6[a]	3.6[a]	3.6[a]
q^{298}	0	2[a]	2[a]	2[a]	1[a]

[a]Parameters fixed during the fitting procedure. [b]Ref 30.

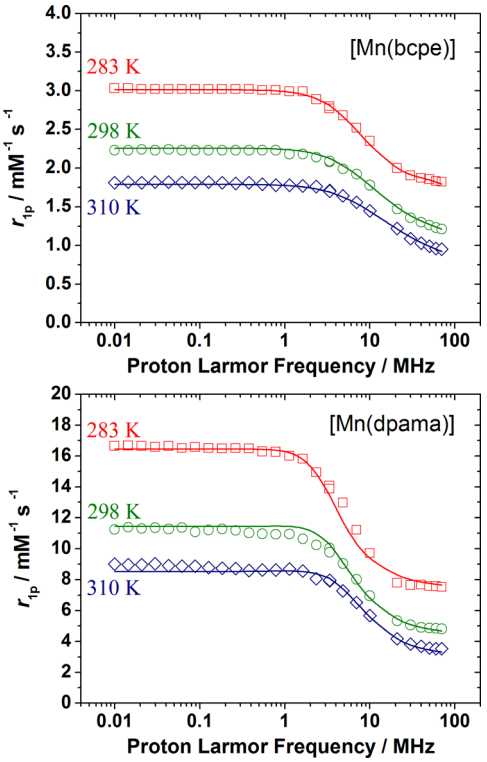

Figure 5. ^{1}H NMRD profiles recorded at different temperatures for [Mn(bcpe)] and [Mn(dpama)]. The lines represent the fit of the data as explained in the text.

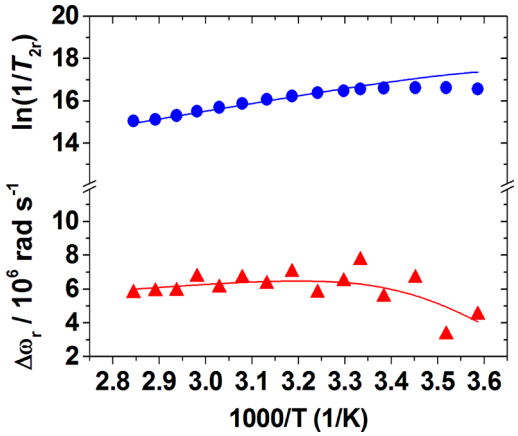

Figure 6. Reduced transverse (blue ●) ^{17}O NMR relaxation rates and ^{17}O NMR chemical shifts (red ▲) versus reciprocal temperature measured for [Mn(dpama)] at 11.74 T. The lines represent the fit of the data as explained in the text.

independent information about some important parameters that control ^{1}H relaxivity, especially the exchange rate of the coordinated water molecule(s) (k_{ex}^{298}). The $1/T_{2r}$ values increase with decreasing temperature, which is typical of systems in the fast-exchange regime. However, the changeover between the fast and slow exchange regimes can be observed in the temperature dependence of the chemical shifts (Figure 6), as also observed for the [Mn(edta)]$^{2-}$ complex.[30]

The ^{1}H NMRD profiles of [Mn(bcpe)] were analyzed by using the Freed model,[32] which accounts for the outer-sphere contribution to relaxivity. The distance of closest approach for the outer-sphere contribution a_{MnH} was fixed at 3.6 Å, while the remaining parameters were allowed to refine freely during the fitting procedure. The parameters characterizing the electron spin relaxation, the electronic correlation time for the modulation of the zero-field-splitting interaction (τ_V), its activation energy (E_V), and the mean square zero-field-splitting energy (Δ^2) take values that are similar to those reported for [Mn(edta)]$^{2-}$ and other Mn^{2+} complexes.[30,33] Furthermore, the values obtained for the diffusion coefficient, D_{MnH}^{298}, and its activation energy, E_{DMnH}, are close to those reported for the self-diffusion of water molecules in pure water (2.3×10^{-9} m^2·s^{-1} and 17.3 kJ mol^{-1}).[34] Thus, we conclude that the value of 3.6 Å assumed for a_{MnH} is reasonable.

A simultaneous fitting of the ^{1}H NMRD and ^{17}O NMR data of [Mn(dpama)] was carried out by taking into account both the outer- and inner-sphere contributions to relaxivity (see Supporting Information for details). In line with the results obtained for [Mn(bcpe)], the distance of closest approach for the outer-sphere contribution a_{MnH} was fixed at 3.6 Å during the fitting procedure, while D_{MnH}^{298} and E_{DMnH} were set to the values obtained for the self-diffusion of water molecules in pure water. Furthermore, the distance between the proton nuclei of the coordinated water molecules and the Mn^{2+} ion (r_{MnH}) was fixed at 2.74 Å, which corresponds to the average Mn···H distance obtained from our DFT calculations presented in a preliminary communication.[16] The number of water molecules in the inner coordination sphere of Mn^{2+} was fixed to q = 2.

DOI: 10.1021/acs.inorgchem.5b01677
Inorg. Chem. 2015, 54, 9576−9587

The parameters obtained from the fittings are listed in Table 4, while the curve fits are shown in Figures 5 and 6.

The water exchange rate determined for [Mn(dpama)] (k_{ex}^{298} = 3.1 × 10^8 s^{-1}) is similar to that reported for $[Mn(edta)(H_2O)]^{2-}$ (k_{ex}^{298} = 4.7 × 10^8 s^{-1})[30] and 1 order of magnitude faster than that determined for the aquated ion $[Mn(H_2O)_6]^{2+}$ (k_{ex}^{298} = 2.8 × 10^7 s^{-1}).[29] The value obtained for the ^{17}O hyperfine coupling constant ($A_O/\hbar$ = −45.8 × 10^6 $rads^{-1}$) is similar to those typically observed for Mn^{2+} complexes (−31 × 10^6 to −43 × 10^6 rad·s^{-1}).[35] Theoretical DFT calculations carried out following our previously reported methodology[20,29] (see Computational section for details) provide A_{iso} values of −48.1 × 10^6 and −52.5 × 10^6 rad·s^{-1} for the two coordinated water molecules, which present nearly identical Mn−O distances (2.206 and 2.205 Å). The excellent agreement between the experimental and calculated $A_O/\hbar$ values clearly confirms that the [Mn(dpama)] presents two coordinated water molecules.

The ^1H NMRD profiles of the $[mX(Mn(dpama)(H_2O)_2)_2]$ and $[mX(Mn(dpama)(H_2O)_2)_3]$ complexes were also recorded at different temperatures (Figure 7). The relaxivities measured

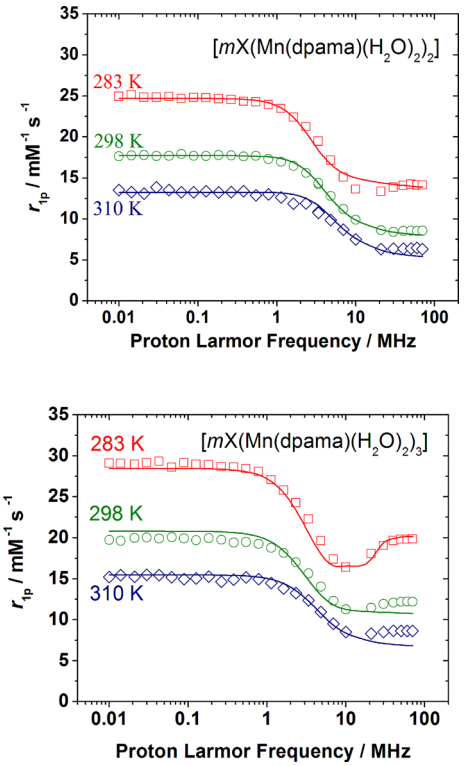

Figure 7. ^1H NMRD profiles recorded at different temperatures for $[mX(Mn(dpama)(H_2O)_2)_2]$ and $[mX(Mn(dpama)(H_2O)_2)_3]$. The lines represent the fit of the data as explained in the text.

at high fields (>20 MHz) for the mono-, bi-, and trinuclear complexes follow a linear correlation (R^2 > 0.9999) with their molecular weight (Figure S10, Supporting Information). At high fields the rotational dynamics (τ_R) plays a major role in determining the relaxivity because both the exchange lifetime (τ_M) and the electronic relaxation times are much longer than τ_R. The ^1H NMRD profiles recorded at three temperatures could be fitted by fixing the structural parameters and those related to diffusion and water exchange to the values obtained for [Mn(dpama)] (Table 4). Thus, only four parameters were allowed to vary during the fitting procedure: τ_R, E_r, τ_v, and Δ^2. Reasonably good fits of the relaxivity data were obtained using this procedure, which suggests that the water exchange of coordinated water molecules does not vary significantly in this series of complexes. The results of the fits indeed show that increasingly long τ_R values are mainly responsible for the increase of relaxivity with molecular weight.

Human Serum Albumin Binding Studies. We recently reported that, due to the presence of hydrophobic functionalities, the monomeric and dimeric complexes [Mn(dpama)] and $[mX(Mn(dpama)(H_2O)_2)_2]$ are able to form noncovalent adducts with HSA.[16] The binding with plasma proteins is typically exploited for increasing the lifetime of the paramagnetic probe in the vascular system, and it is accompanied by a relaxivity enhancement arising from the reduced tumbling motion of the probe (lengthening of τ_R).[36] [Mn(dpama)] showed a fairly good affinity for HSA (K_A = 3372 ± 138 M^{-1}) but a quite modest relaxivity in the bound form (r_{1p}^b = 12.2 ± 0.8 mM^{-1} s^{-1}), suggesting the displacement of the inner-sphere water molecules by donor groups of the protein at the binding site. On the other hand, $[mX(Mn(dpama)(H_2O)_2)_2]$ is characterized by a strong relaxivity enhancement upon binding to HSA (r_{1p}^b = 39.0 ± 1.3 mM^{-1} s^{-1}) explained by the interaction of the ditopic complex with the hydrophobic site of the protein through one [Mn(dpama)] unit (whose Mn has q = 0), while leaving the other unit exposed to the solvent (q = 2).

The binding interaction of $[mX(Mn(dpama)(H_2O)_2)_3]$ has been investigated through the well-established proton relaxation enhancement (PRE) technique. This consists in measuring the increase of the water proton longitudinal relaxation rate (R_1) of a dilute solution of the complex as a function of increasing concentration of the protein at a given frequency and temperature. The fitting of the experimental data to the PRE equations provides the values of the thermodynamic association constant, K_A, the number of the equivalent and independent binding sites, n, and the relaxivity of the bound complex, r_1^b. Similarly to several previous cases, the data were fitted to a 1:1 binding isotherm even though the presence of multiple affinity sites on HSA cannot be excluded. Titration of a 0.055 mM solution of $[mX(Mn(dpama)(H_2O)_2)_3]$ with HSA (pH = 7.2, 20 MHz, and 310 K) confirmed the binding of the complex to the protein with an association constant of 1286 ± 55 M^{-1} (Figure 8; Table 5), a value very similar to that assessed for the dinuclear derivative. As for $[mX(Mn(dpama)(H_2O)_2)_2]$, also

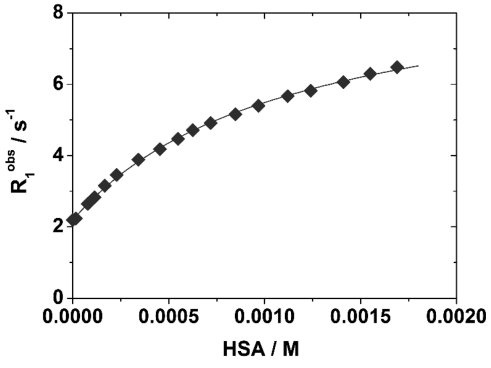

Figure 8. Plot of the water proton longitudinal relaxation rate of a solution of $[mX(Mn(dpama)(H_2O)_2)_3]$ (0.055 mM) as a function of HSA concentration at 20 MHz, 310 K, and pH = 7.2. The line through the data has been calculated with the parameters of Table 5.

DOI: 10.1021/acs.inorgchem.5b01677
Inorg. Chem. 2015, 54, 9576−9587

Table 5. Best-Fit Parameters Obtained from the Analysis of the ^{1}H Relaxometric Titrations (20 MHz; 310 K) of the Mn^{2+} Complexes with HSA[a]

	dpama^{2-}	mX(dpama)$_2^{4-}$	mX(dpama)$_3^{6-}$
$n{\cdot}K_A$ (M^{-1})	3372 ± 138	1125 ± 35	1286 ± 85
r_{1p}^b (mM^{-1} s^{-1})	12.2 ± 0.8	39.0 ± 1.3	45.2 ± 0.6
r_{1p}^f (mM^{-1} s^{-1})[b]	4.2	6.1	8.3

[a]Data for dpama^{2-} and mX(dpama)$_2^{4-}$ from ref 16. [b]r_{1p}^f is the relaxivity of the free complex.

the relaxivity of the adduct (45.2 ± 0.6 mM^{-1} s^{-1}) is remarkably high, in line with the reasonable assumption that also in this case a single chelating unit is involved in the binding, while the other two are freely accessible to solvent and responsible for the relaxivity increase. The value of r_1^b is the average relaxivity per Mn^{2+} ion, while the molecular relaxivity (per complex) is 135.6 mM^{-1} s^{-1}. If we assume for the unit with q = 0 (that is embedded in the hydrophobic pocket of HSA) the same value of r_1^b found per [Mn(dpama)], then each q = 2 unit is characterized by a relaxivity of about 62 mM^{-1} s^{-1}. This value is quite comparable to that calculated previously for [mX(Mn(dpama)$(H_2O)_2)_2$]$_2$].

The NMRD profile has been measured for a 0.055 mM solution of the trinuclear complex in the presence of 1.7 mM HSA at 310 K. Under these conditions, ca. 68% of the complex is bound to the protein. The calculated profile corresponding to the fully bound form is reported in Figure 9 (the r_1^b values are

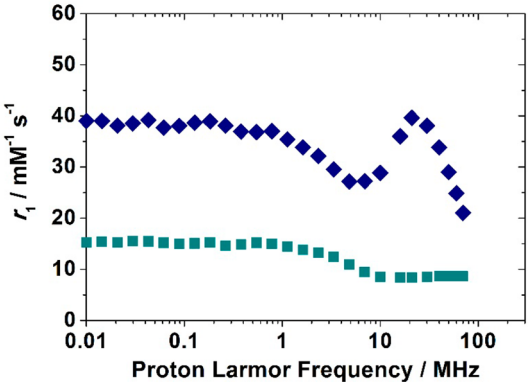

Figure 9. ^{1}H NMRD profiles for [mX(Mn(dpama)$(H_2O)_2)_3$] free (bottom) and fully bound to HSA (top) at 310 K and pH = 7.2.

expressed per Mn) and is characteristic of a slowly tumbling system with a pronounced peak around 30 MHz and a large relaxivity enhancement over the free complex due to the slow rotation and fast exchange conditions (long τ_R and short τ_M values).

CONCLUSIONS

We have reported a series of ligands containing pentadentate coordinating units designed for pentagonal bipyramidal coordination around Mn^{2+} due to the presence of two coordinated water molecules. This imparts remarkably high relaxivities to the solutions of the corresponding Mn^{2+} complexes. Furthermore, these relaxivities are further improved by interaction with HSA, particularly in the case of the trinuclear Mn^{2+} complex. This property is very interesting for MRI visualization of blood vessels, as well as to improve the residence time of the agent in the blood pool. The Mn^{2+} complexes formed with this family of ligands present moderate thermodynamic stabilities. Although this may not be a very serious limitation due to the far better safety profile of Mn^{2+} compared to Gd^{3+}, we intend to design and develop Mn^{2+} complexes that, while maintaining these favorable relaxometric properties, exhibit improved characteristics of kinetic inertness with respect to complex dissociation.

EXPERIMENTAL AND COMPUTATIONAL SECTION

Materials and Methods. H_2bcpe, H_2dpama, and mX(H_2dpama)$_2$ were prepared following the published syntheses.[16,17] Benzene-1,3,5-triyltrimethanamine (**1**) was prepared from 1,3,5-tris(bromomethyl)-benzene in two steps involving the reaction of the latter with NaN_3 followed by catalytic hydrogenation of the azide intermediate.[37] All other chemicals were purchased from commercial sources and used without further purification, unless otherwise stated. Elemental analyses were carried out on a Carlo Erba 1108 elemental analyzer. ESI-TOF mass spectra were recorded using a LC-Q-q-TOF Applied Biosystems QSTAR Elite spectrometer in the positive mode. IR spectra were recorded on a Bruker Vector 22 instrument with an ATR accessory. ^{1}H and ^{13}C NMR spectra were recorded at 25 °C on a Bruker Avance 500 MHz spectrometer.

The stock solutions of $MnCl_2$, $ZnCl_2$, and $CuCl_2$ used for equilibrium measurements were prepared by dissolving $MnCl_2$, $ZnCl_2$, and $CuCl_2$ (Fluka 99.9%) in water. The concentrations of the solutions were determined by complexometric titrations with standardized Na_2H_2EDTA and eriochrome black T ($MnCl_2$), xylenol orange ($ZnCl_2$), and murexide ($CuCl_2$) as indicators.[38] The concentration of the H_2bcpe, H_2dpama, mX(H_2dpama)$_2$, and mX(H_2dpama)$_3$ ligand solutions was determined by pH-potentiometric titrations in the presence and absence of a 40-fold excess of Ca(II). The pH-potentiometric titrations were performed with standardized 0.2 M NaOH.

Equilibrium Measurements. All the equilibrium measurements were conducted at a constant ionic strength maintained by 0.15 M NaCl at 298 K. For determining the protonation constants of the bcpe^{2-}, dpama^{2-}, mX(dpama)$_2^{4-}$, and mX(dpama)$_3^{6-}$ ligands pH-potentiometric titrations were performed with 0.2 M NaOH using 0.002 M ligand solutions. The stability and protonation constants of Mn^{2+} and Zn^{2+} complexes were determined by pH-potentiometric titrations. The metal to ligand concentration ratios were 1:1 for bcpe^{2-} and dpama^{2-}, 1:1 and 2:1 for mX(dpama)$_2^{4-}$, and 1:1, 2:1, and 3:1 for mX(dpama)$_3^{6-}$ (the concentration of the ligand was generally 0.002 M). Because the formation and dissociation reactions of the Mn^{2+} and Zn^{2+} complexes are fast in the pH range 1.7−4.0 (at pH > 4 fast deprotonation reactions of the protonated complexes take place in all systems), the titration rate of Mn^{2+}−L and Zn^{2+}−L samples was carried out with an addition rate of 0.01 mL base/min. For the calculation of the equilibrium constants the mL base−pH data obtained with 1.1 stoichiometry were used, obtained in the pH range 1.7−12.0. The equilibrium constants characterizing the Mn^{2+}−mX(dpama)$_2^{4-}$ and Mn^{2+}−mX(dpama)$_3^{6-}$ systems were calculated by the simultaneous fitting of the pH-potentiometric data sets (V−pH) obtained at 1:1 and 2:1 (Mn^{2+}−mX(dpama)$_2^{4-}$) and 1:1, 2:1, and 3:1 Mn^{2+}−mX(dpama)$_3^{6-}$) metal to ligand concentration ratios ($3\sigma \leq$ 0.005 mL). The pH-potentiometric titrations were carried out using a 785 DMP Titrino titration workstation with the use of a Metrohm-6.0233.100 combined electrode. The titrated solution (8 mL) was thermostated at 25 °C. The samples were stirred, and to avoid the effect of CO_2, N_2 gas was bubbled through the solutions. For the calibration of the pH meter, KH-phthalate (pH = 4.002) and borax (pH = 8.970) buffers were used. For the calculation of the H^+ concentration from the measured pH values, the method proposed by Irving et al. was used.[39] A 0.01 M HCl (0.15 M NaCl) solution was titrated with 0.2 M NaOH, and the difference between the measured and calculated pH values was used to calculate [H^+] from the pH values determined in the titration experiments.

The stability constants of the [Cu(bcpe)] and [Cu(dpama)] complexes have been determined by spectrophotometry, with the use

DOI: 10.1021/acs.inorgchem.5b01677
Inorg. Chem. 2015, 54, 9576−9587

of the competition reactions taking place between the concerned ligand ($bcpe^{2-}$ or $dpama^{2-}$) and $egta^{4-}$ for Cu^{2+} complexation in the pH range 6.8−7.2. The concentration of Cu^{2+} and $bcpe^{2-}$ (or $dpama^{2-}$) in the eight samples was 3 mM, while the concentration of egta was varied between 0 and 8 mM. The molar absorptivities of $CuCl_2$ and the complexes [Cu(dpama)], [Cu(bcpe)], and $[Cu(egta)]^{2-}$ were determined in 1.5, 3.0, and 4.5 mM solutions. The absorbance and pH values were determined in the samples after the equilibrium was reached. The time needed to reach the equilibrium in these systems was determined by spectrophotometry and found to be 3 weeks. Spectrophotometric measurements were made between 700 and 800 nm at 11 wavelength values. The spectrophotometric measurements were recorded with the use of 1.0 cm cells using a Cary 1E spectrophotometer at 298 K. The data sets obtained by pH-potentiometry (V−pH) and by spectrophotometry (Abs−pH) were used for the calculation of the equilibrium constants with the aid of the PSEQUAD program.[40]

Cyclic Voltammetry. Cyclic voltammograms were recorded using a 797 VA Computrace potentiostat/galvanostat from Metrohm (Herisau, Switzerland) using a typical three-electrode cell. A glassy carbon rotating disk electrode (RDE) was used as working electrode. The counter electrode was a platinum rod electrode. Potentials were measured using a Ag/AgCl reference electrode filled with 3 mol·L^{-1} KCl. A stirring rate of 2000 rpms was used in the RDE. Solutions were purged with high-purity (99.999%) nitrogen during 30 s prior to recording the voltammograms. The starting and end potentials were 0.0 V, while the first vertex potential was set to +1.0 V.

^{1}H NMRD and ^{17}O NMR Measurements. The water proton longitudinal relaxation rates as a function of pH (20 MHz) were measured with a Stelar Spinmaster FFC-2000 spectrometer (Mede, PV, Italy) on about 0.6−2.0 mM aqueous solutions in nondeuterated water. The exact concentrations of Mn^{2+} ions were determined by measurement of bulk magnetic susceptibility shifts of a *t*BuOH signal on a Bruker Avance III spectrometer (11.7 T). The ^{1}H T_1 relaxation times were acquired by the standard inversion recovery method with a typical 90° pulse width of 3.5 μs and 16 experiments of four scans. The reproducibility of the T_1 data was ±5%. The temperature was controlled with a Stelar VTC-91 airflow heater equipped with a calibrated copper−constantan thermocouple (uncertainty of ±0.1 °C). The proton $1/T_1$ NMRD profiles were measured on a fast field-cycling Stelar SmartTracer relaxometer over a continuum of magnetic field strengths of 0.00024−0.25 T (corresponding to 0.01−10 MHz proton Larmor frequencies). The relaxometer operates under computer control with an absolute uncertainty in $1/T_1$ of ±1%. Additional data points in the range 15−70 MHz were obtained on a Stelar relaxometer equipped with a Bruker WP80 NMR electromagnet adapted to variable-field measurements (15−80 MHz proton Larmor frequency).

Variable-temperature ^{17}O NMR measurements were recorded on a Bruker Avance III spectrometer (11.7 T) equipped with a 5 mm probe and standard temperature control unit. An aqueous solution of the complex (4 mM) containing 2.0% of the ^{17}O isotope (Cambridge Isotope) was used. The observed transverse relaxation rates were calculated from the signal width at half-height.

*Hexaethyl 6,6′,6″,6‴,6⁗,6⁗′-(((benzene-1,3,5-triyltris-(methylene))tris (azanetriyl))hexakis(methylene))hexapicolinate (**3**).* 6-Chloromethylpyridine-2-carboxylic acid ethyl ester **2** (2.67 g, 13.4 mmol) and K_2CO_3 (2.95 g, 21.3 mmol) were added to a solution of benzene-1,3,5-triyltrimethanamine[37] (0.356 g, 2.15 mmol) in acetonitrile (150 mL). The mixture was stirred for a period of 5 days at room temperature and then 7 days at 45 °C. The excess K_2CO_3 was filtered off, the filtrate was concentrated to dryness, and the yellow residue was extracted with 200 mL of a $H_2O/CHCl_3$ (1:3) mixture. The organic phase was evaporated to dryness to give an oily residue, which was purified by column chromatography on neutral Al_2O_3 with a CH_2Cl_2/MeOH mixture as the eluent (gradient 0% to 3% of MeOH) to give 1.30 g of **3** as a yellow oil. Yield: 53%. Anal. Calcd for $C_{63}H_{69}N_9O_{12}$: C, 66.13; H, 6.08; N, 11.02. Found: C, 65.84; H, 5.98; N, 11.12. HR-MS (ESI$^+$, CH_3CN): m/z 1144.5115; calcd for $[C_{63}H_{70}N_9O_{12}]^+$ 1144.5138. IR (ATR): ν 1714 cm^{-1} (C═O). ^{1}H NMR ($CDCl_3$, 500 MHz, 25 °C, TMS): δ 7.95 (m, 6H), 7.77 (m, 12H), 7.33 (s, 3H), 4.44 (c, 12H, ^3J = 7.1 Hz), 3.91 (s, 12H), 3.71 (s, 6H), 1.40 ppm (t, 18H, ^3J = 7.1 Hz). ^{13}C NMR ($CDCl_3$, 125.8 MHz, 25 °C, TMS): δ 165.2, 160.3, 147.7, 139.0, 137.4, 128.3, 125.7, 123.5, 61.8, 59.7, 58.6, 14.3 ppm.

6,6′,6″,6‴,6⁗,6⁗′-(((Benzene-1,3,5-triyltris(methylene))tris-(azanetriyl)) hexakis(methylene))hexapicolinic acid (mX-(H_2dpama)$_3$·9HCl). A solution of compound **3** (1.30 g, 1.14 mmol) in 6 M HCl (50 mL) was heated to reflux for 24 h, and then the solvent was removed in a rotary evaporator to give a yellow oil. A small amount of H_2O was added (∼10 mL), which resulted in the precipitation of a white solid. It was collected by filtration, washed with H_2O (∼5 mL) and acetone (∼5 mL), and dried under vacuum to give 1.02 g of the desired ligand as a white solid. Yield: 69%. Anal. Calcd for $C_{51}H_{45}N_9O_{12}$·9HCl: C, 46.97; H, 4.17; N, 9.67. Found: C, 46.99; H, 3.99; N, 9.51. MS (ESI$^+$, H_2O): m/z 976 ($[C_{51}H_{46}N_9O_{12}]^+$). IR (ATR): ν 1752 and 1733 cm^{-1} (C═O). ^{1}H NMR (D_2O, pD 7.0, 500 MHz, 25 °C, TMS): δ 7.51 (m, 12H), 7.36 (s, 3H), 7.20 (m, 6H), 4.15 (s, 12H), 4.12 ppm (s, 6H). ^{13}C NMR (D_2O, pD 7.0, 125.8 MHz, 25 °C, TMS): δ 171.8, 152.5, 152.3, 138.5, 133.9, 132.7, 125.7, 123.1, 59.3, 58,9 ppm.

Preparation of the Complex [mX(Mn(dpama)(H_2O)$_2$)$_3$]·11H_2O. A solution of *m*X(H_2dpama)$_3$·9HCl (0.100 g, 0.077 mmol), triethylamine (0.116 g, 1.15 mmol), and $MnCl_2$·4H_2O (0.046 g, 0.231 mmol) in 2-propanol (10 mL) was stirred at room temperature for 24 h under an argon atmosphere. The white solid formed was isolated by filtration and then suspended in acetonitrile (10 mL) and stirred at room temperature for 24 h. The solid was isolated by filtration, washed with acetonitrile and diethyl ether, and dried under vacuum. Yield: 0.066 g, 59%. Anal. Calcd for $C_{51}H_{39}Mn_3N_9O_{12}$·17$H_2O$: C, 42.51; H, 5.11; N, 8.75. Found: C, 42.69; H, 5.02; N, 8.75. HR-MS (ESI$^+$, MeOH/H_2O, 1:1): m/z 590.0354; calcd for $[C_{51}H_{39}Mn_3N_9Na_2O_{12}]^{2+}$ 590.0321. IR (ATR, cm^{-1}): ν 1622 and 1586 (C═O).

[Mn(bcpe)]·3H_2O. A solution of H_2bcpe·8HCl[17] (0.100 g, 0.161 mmol), triethylamine (0.163 g, 1.61 mmol), and $Mn(ClO_4)_2$·6H_2O (0.058 g, 0.161 mmol) in a mixture of 2-propanol and MeOH (9:1, 10 mL) was stirred at room temperature for 24 h under an argon atmosphere, which resulted in the formation of a white solid. This was isolated by filtration, washed with 2-propanol and diethyl ether, and dried under vacuum. Yield: 0.042 g, 60%. Anal. Calcd for $C_{16}H_{16}MnN_4O_4$·3H_2O: C, 43.94; H, 5.07; N, 12.81. Found: C, 43.74; H, 5.35; N, 12.65. HR-MS (ESI$^+$, MeOH/CH_3CN/H_2O, 9:1:1): m/z 384.0628; calcd for $[C_{16}H_{17}MnN_4O_4]^+$ 384.0624. IR (ATR, cm^{-1}): ν 1625 and 1590 (C═O).

X-ray Crystallography. Three dimensional X-ray data were collected on a Bruker Kappa APEXII CCD diffractometer. Data were corrected for Lorentz and polarization effects and for absorption by semiempirical methods[41] based on symmetry-equivalent reflections. Complex scattering factors were taken from the program SHELX2013[42] included in the WinGX program system[43] as implemented on a Pentium computer. The structure was solved by Patterson methods (DIRDIF2008)[44] and refined[42] by full-matrix least-squares on F^2. All hydrogen atoms were included in calculated positions and refined in riding mode, except those of the water molecules, which were located in a difference electron-density map and the usual restraints applied (DFIX 0.84(1) and DANG 1.34(2)). Refinement converged with anisotropic displacement parameters for all non-hydrogen atoms. Both water molecules present in the crystal show positional disorders that have been solved; the first water molecule was disordered in three positions, and the total occupancy factor was restrained to 1 with SUMP. The occupancy factors obtained for the three positions were 0.218(2) for O5A, 0.609(2) for O5B, and 0.174(2) for O5C. The second water molecule was disordered in two positons with occupancy factors of 0.23(2) for O6A and 0.77(2) for O6B. Crystal data and details on data collection: yellow prism (0.32 × 0.30 × 0.15 mm) crystals of $C_{16}H_{20}MnN_4O_6$, M = 419.30, monoclinic, a = 10.7431(11) Å, b = 10.4863(10) Å, c = 10.0766(18) Å, β = 95.271(5), V = 1803.5(3) Å^3, Z = 4, space group: $P2_1/n$ (No. 14), ρ_{calc} = 1.544 g cm^{-3}. θ_{max} = 26.44°, 17 277 measured reflections, of which 3706 were independent and 3313 were unique with $I > 2\sigma(I)$, R1 =

DOI: 10.1021/acs.inorgchem.5b01677
Inorg. Chem. 2015, 54, 9576−9587

0.0306 and wR2 (all data) = 0.0847. Residual electron density: 0.559/−0.317 e/Å^3.

Computational Details. All calculations presented in this work were performed employing the Gaussian 09 package (revision D.01).[45] Full geometry optimizations of the $[m\mathrm{X}(\mathrm{Mn}(\mathrm{dpama})(\mathrm{H_2O}))_3]\cdot 12\mathrm{H_2O}$ system were performed in aqueous solution employing DFT within the hybrid meta generalized gradient approximation (hybrid meta-GGA) with the TPSSh exchange−correlation functional[46] and the standard Ahlrich's double-ξ basis set with polarization functions (SVP).[47] No symmetry constraints have been imposed during the optimizations. Due to the large effort involving the calculation of second derivatives for such a large system, no frequency analysis was performed. The isotropic ^{17}O and ^{1}H hyperfine coupling constants (A_{iso} values) of the $[\mathrm{Mn}(\mathrm{dpama})(\mathrm{H_2O})_2]\cdot 4\mathrm{H_2O}$ system were calculated in aqueous solution using the TPSSh exchange−correlation functional and the geometry described in our previous communication.[16] For the description of C, H, N, and O atoms we used the EPR-III basis set of Barone,[48] which is a triple-ζ basis set including diffuse functions, double d-polarizations, and a single set of f-polarization functions, together with an improved s-part to better describe the nuclear region. For Mn we used the aug-cc-pVTZ-J basis set developed by Sauer for the calculation of EPR parameters, which possesses a (25s17p10d3f2g)/[17s10p7d3f2g] contraction scheme and contains four tight s-, one tight p-, and one tight d-type function.[49] Solvent effects were included by using the polarizable continuum model (PCM), in which the solute cavity is built as an envelope of spheres centered on atoms or atomic groups with appropriate radii. In particular, the integral equation formalism (IEFPCM) variant as implemented in Gaussian 09 was used.[50]

■ ASSOCIATED CONTENT

Supporting Information

The Supporting Information is available free of charge on the ACS Publications website at DOI: 10.1021/acs.inorgchem.5b01677.

^{1}H and ^{13}C NMR, high-resolution mass spectra, species distribution diagrams, plots of relaxivity as a function of pH and molecular weight, and optimized Cartesian coordinates obtained with DFT calculations (PDF)

Crystallographic data (CIF)

■ AUTHOR INFORMATION

Corresponding Authors

*E-mail: mauro.botta@uniupo.it.

*E-mail: carlos.platas.iglesias@udc.es.

Notes

The authors declare no competing financial interest.

■ ACKNOWLEDGMENTS

M.R.-F., D.E.-G., A.deB., T.R.-B., and C.P.-I. thank Xunta de Galicia (CN 2012/011) and Universidade da Coruña for generous financial support and Centro de Supercomputación de Galicia (CESGA) for providing the computer facilities. M.B. acknowledges the MIUR (PRIN 2012: "Innovative chemical tools for improved molecular approaches in biomedicine") for financial support.

■ REFERENCES

(1) (a) Yang, C.-T.; Chuang, K.-H. *MedChemComm* **2012**, *3*, 552−565. (b) Caravan, P.; Ellison, J.; McMurry, T.; Lauffer, R. *Chem. Rev.* **1999**, *99*, 2293−2352. (c) Terreno, E.; Castelli, D. D.; Viale, A.; Aime, S. *Chem. Rev.* **2010**, *110*, 3019−3042. (d) De Leon-Rodriguez, L. M.; Lubag, A. J. M.; Malloy, C. R.; Martinez, G. V.; Gillies, R. J.; Sherry, A. D. *Acc. Chem. Res.* **2009**, *42*, 948−957. (e) Butler, S. J.; Parker, D. *Chem. Soc. Rev.* **2013**, *42*, 1652−1666. (f) Boros, E.; Gale, E. M.; Caravan, P. *Dalton Trans.* **2015**, *44*, 4804−4818. (g) Viswanathan, S.; Kovacs, Z.; Green, K. N.; Ratnakar, S. J.; Sherry, A. D. *Chem. Rev.* **2010**, *110*, 2960−3018.

(2) *The Chemistry of Contrast Agents in Medical Magnetic Resonance Imaging*, Second ed.; Merbach, A. E.; Helm, L.; Tóth, É., Eds.; Wiley: New York, 2013.

(3) Pierre, V. C.; Allen, M. J.; Caravan, P. *JBIC, J. Biol. Inorg. Chem.* **2014**, *19*, 127−131.

(4) (a) Kueny-Stotz, M.; Garofalo, A.; Felder-Flesch, D. *Eur. J. Inorg. Chem.* **2012**, *2012*, 1987−2005. (b) Drahos, B.; Lukes, I.; Toth, E. *Eur. J. Inorg. Chem.* **2012**, *2012*, 1975−1986. (c) Pan, D.; Schmieder, A. H.; Wickline, S. A.; Lanza, G. M. *Tetrahedron* **2011**, *67*, 8431−8444.

(5) (a) Kuznik, N.; Szafraniec-Gorol, G.; Oczek, L.; Grucela, A.; Jewula, P.; Kuznik, A.; Zassowski, P.; Domagala, W. *J. Organomet. Chem.* **2014**, *769*, 100−105. (b) Su, H.; Wu, C.; Zhu, J.; Miao, T.; Wang, D.; Xia, C.; Zhao, X.; Gong, Q.; Song, B.; Ai, H. *Dalton Trans.* **2012**, *41*, 14480−14483.

(6) Rocklage, S. M.; Cacheris, W. P.; Quay, S. C.; Hahn, F. E.; Raymond, K. N. *Inorg. Chem.* **1989**, *28*, 477−485.

(7) Geraldes, C. F. G. C.; Sherry, A. D.; Brown, R. D., III; Koenig, S. H. *Magn. Reson. Med.* **1986**, *3*, 242−250.

(8) (a) Rief, M.; Asbach, P.; Franiel, T.; Taupitz, M.; Hamm, B.; Wagner, M. *Contrast Media Mol. Imaging* **2009**, *4*, 267−268. (b) Albiin, N.; Kartalis, N.; Bergquist, A.; Sadigh, B.; Brismar, T. B. *MAGMA* **2012**, *25*, 361−368.

(9) Karlsson, J. O. G.; Ignarro, L. J.; Lundström, I.; Jynge, P.; Almén, T. *Drug Discovery Today* **2015**, *20*, 41110.1016/j.drudis.2014.11.008

(10) Caravan, P.; Farrar, C. T.; Frullano, L.; Uppal, R. *Contrast Media Mol. Imaging* **2009**, *4*, 89−100.

(11) (a) Baranyai, Z.; Botta, M.; Fekete, M.; Giovenzana, G. B.; Negri, R.; Tei, L.; Platas-Iglesias, C. *Chem. - Eur. J.* **2012**, *18*, 7680−7685. (b) Negri, R.; Baranyai, Z.; Tei, L.; Giovenzana, G. B.; Platas-Iglesias, C.; Bényei, A. C.; Bodnár, J.; Vágner, A.; Botta, M. *Inorg. Chem.* **2014**, *53*, 12499−12511. (c) Aime, S.; Gianolio, E.; Corpillo, D.; Cavallotti, C.; Palmisano, G.; Sisti, M.; Giovenzana, G. B.; Pagliarin, R. *Helv. Chim. Acta* **2003**, *86*, 615−632. (d) Aime, S.; Calabi, L.; Cavallotti, C.; Gianolio, E.; Giovenzana, G. B.; Losi, P.; Maiocchi, A.; Palmisano, G.; Sisti, M. *Inorg. Chem.* **2004**, *43*, 7588−7590. (e) Costa, J.; Tóth, É.; Helm, L.; Merbach, A. E. *Inorg. Chem.* **2005**, *44*, 4747−4755. (f) Moriggi, L.; Cannizzo, C.; Prestinari, C.; Berrière, F.; Helm, L. *Inorg. Chem.* **2008**, *47*, 8357−8366. (g) Gale, E. M.; Kenton, N.; Caravan, P. *Chem. Commun.* **2013**, *49*, 8060−8062.

(12) Drahos, B.; Kotek, J.; Hermann, P.; Lukes, I.; Toth, E. *Inorg. Chem.* **2010**, *49*, 3224−3238.

(13) (a) Loving, G. S.; Mukherjee, S.; Caravan, P. *J. Am. Chem. Soc.* **2013**, *135*, 4620−4623. (b) Gale, E. M.; Mukherjee, S.; Liu, C.; Loving, G. S.; Caravan, P. *Inorg. Chem.* **2014**, *53*, 10748−10761.

(14) Tsitovich, P. B.; Burns, P. J.; McKay, A. M.; Morrow, J. R. *J. Inorg. Biochem.* **2014**, *133*, 143−154.

(15) Aime, S.; Botta, M.; Gianolio, E.; Terreno, E. *Angew. Chem., Int. Ed.* **2000**, *39*, 747−750.

(16) Regueiro-Figueroa, M.; Rolla, G. A.; Esteban-Gómez, D.; de Blas, A.; Rodríguez-Blas, T.; Botta, M.; Platas-Iglesias, C. *Chem. - Eur. J.* **2014**, *20*, 17300−17305.

(17) Ferreirós-Martínez, R.; Esteban-Gómez, D.; Platas-Iglesias, C.; de Blas, A.; Rodríguez-Blas, T. *Dalton Trans.* **2008**, 5754−5765.

(18) Boros, E.; Ferreira, C. L.; Cawthray, J. F.; Price, E. W.; Patrick, B. O.; Wester, D. W.; Adam, M. J.; Orvig, C. *J. Am. Chem. Soc.* **2010**, *132*, 15726−15733.

(19) Boros, E.; Cawthray, J. F.; Ferreira, C. L.; Patrick, B. O.; Adam, M. J.; Orvig, C. *Inorg. Chem.* **2012**, *51*, 6279−6284.

(20) (a) Molnar, E.; Camus, N.; Patinec, V.; Rolla, G. A.; Botta, M.; Tircso, G.; Kalman, F. K.; Fodor, T.; Tripier, R.; Platas-Iglesias, C. *Inorg. Chem.* **2014**, *53*, 5136−5149. (b) Patinec, V.; Rolla, G. A.; Botta, M.; Tripier, R.; Esteban-Gómez, D.; Platas-Iglesias, C. *Inorg. Chem.* **2013**, *52*, 11173−11184.

(21) Huang, Q.; Zhai, B. *J. Coord. Chem.* **2007**, *60*, 2257−2263.

(22) Friis, E. P.; Andersen, J. E. T.; Madsen, L. L.; Bonander, N.; Moller, P.; Ulstrup, J. *Electrochim. Acta* **1998**, *43*, 1114−1122.

DOI: 10.1021/acs.inorgchem.5b01677
Inorg. Chem. 2015, 54, 9576−9587

(23) Crowley, J. D.; Traynor, D. A.; Weatherburn, D. C. In *Metal Ions in Biological Systems*: Vol. 37; Sigel, A.; Sigel, H., Eds.; Marcel Dekker: New York, 2000; Chapter 8, p 214.
(24) Jons, O.; Johansen, E. S. *Inorg. Chim. Acta* **1988**, *151*, 129−132.
(25) Benson, S. W. *J. Am. Chem. Soc.* **1958**, *80*, 5151−5154.
(26) Artali, R.; Baranyai, Z.; Botta, M.; Giovenzana, G. B.; Maspero, A.; Negri, R.; Palmisano, G.; Sisti, M.; Tollari, S. *New J. Chem.* **2015**, *39*, 539−547.
(27) Irving, H.; Williams, R. J. P. *J. Chem. Soc.* **1953**, 3192−3210.
(28) Regueiro-Figueroa, M.; Lima, L. M. P.; Blanco, V.; Esteban-Gómez, D.; de Blas, A.; Rodríguez-Blas, T.; Delgado, R.; Platas-Iglesias, C. *Inorg. Chem.* **2014**, *53*, 12859−12869.
(29) Esteban-Gómez, D.; Cassino, C.; Botta, M.; Platas-Iglesias, C. *RSC Adv.* **2014**, *4*, 7094−7103.
(30) Rolla, G. A.; Platas-Iglesias, C.; Botta, M.; Tei, L.; Helm, L. *Inorg. Chem.* **2013**, *52*, 3268−3279.
(31) Balogh, E.; He, Z.; Hsieh, W.; Liu, S.; Toth, E. *Inorg. Chem.* **2007**, *46*, 238−250.
(32) Freed, J. H. *J. Chem. Phys.* **1978**, *68*, 4034−4037.
(33) (a) Drahos, B.; Kotek, J.; Cisarova, I.; Hermann, P.; Helm, L.; Lukes, I.; Toth, E. *Inorg. Chem.* **2011**, *50*, 12785−12801. (b) Drahos, B.; Pniok, M.; Havlickova, J.; Kotek, J.; Cisarova, I.; Hermann, P.; Lukes, I.; Toth, E. *Dalton Trans.* **2011**, *40*, 10131−10146. (c) Tei, L.; Gugliotta, G.; Fekete, M.; Kalman, F.; Botta, M. *Dalton Trans.* **2011**, *40*, 2025−2032.
(34) Mills, R. *J. Phys. Chem.* **1973**, *77*, 685−688.
(35) (a) Gale, E. M.; Zhu, J.; Caravan, P. *J. Am. Chem. Soc.* **2013**, *135*, 18600−18608. (b) Zhu, J.; Gale, E. M.; Atanasova, I.; Rietz, T. A.; Caravan, P. *Chem. - Eur. J.* **2014**, *20*, 14507−14513.
(36) (a) Troughton, J. S.; Greenfield, M. T.; Greenwood, J. M.; Dumas, S.; Wiethoff, A. J.; Wang, J.; Spiller, M.; McMurry, T. J.; Caravan, P. *Inorg. Chem.* **2004**, *43*, 6313−6323. (b) Aime, S.; Anelli, P. L.; Botta, M.; Brocchetta, M.; Canton, S.; Fedeli, F.; Gianolio, E.; Terreno, E. *JBIC, J. Biol. Inorg. Chem.* **2002**, *7*, 58−67.
(37) (a) Cecioni, S.; Argintaru, O.-A.; Docsa, T.; Gergely, P.; Praly, J.-P.; Vidal, S. *New J. Chem.* **2009**, *33*, 148−156. (b) Granzhan, A.; Schouwey, C.; Riis-Johannessen, T.; Scopelliti, R.; Severin, K. *J. Am. Chem. Soc.* **2011**, *133*, 7106−7115.
(38) Beynon, R. J.; Easterby, J. S. In *Buffer Solutions: The Basics*; Oxford University Press: New York, 1996.
(39) Irving, H. M.; Miles, M. G.; Pettit, L. *Anal. Chim. Acta* **1967**, *38*, 475−488.
(40) Zékány, L.; Nagypál, I. In *Computational Method for Determination of Formation Constants*; Legett, D. J., Ed.; Plenum: New York, 1985; p 291.
(41) Sheldrick, G. M. *SADABS* Version 2008/1; Bruker AXS Inc., University of Göttingen: Göttingen, Germany, 2008.
(42) Sheldrick, G. M. *Acta Crystallogr., Sect. A: Found. Crystallogr.* **2008**, *64*, 112−122.
(43) Farrugia, L. J. *J. Appl. Crystallogr.* **1999**, *32*, 837−838.
(44) Beurskens, P. T.; Beurskens, G.; de Gelder, R.; Smits, J. M. M.; Garcia-Granda, S.; Gould, R. O. *DIRDIF2008*; Crystallography Laboratory, Radboud University Nijmegen: Toernooiveld 1, 65525 ED Nijmegen, The Netherlands, 2008.
(45) Frisch, M. J.; Trucks, G. W.; Schlegel, H. B.; Scuseria, G. E.; Robb, M. A.; Cheeseman, J. R.; Scalmani, G.; Barone, V.; Mennucci, B.; Petersson, G. A.; Nakatsuji, H.; Caricato, M.; Li, X.; Hratchian, H. P.; Izmaylov, A. F.; Bloino, J.; Zheng, G.; Sonnenberg, J. L.; Hada, M.; Ehara, M.; Toyota, K.; Fukuda, R.; Hasegawa, J.; Ishida, M.; Nakajima, T.; Honda, Y.; Kitao, O.; Nakai, H.; Vreven, T.; Montgomery, J. A., Jr.; Peralta, J. E.; Ogliaro, F.; Bearpark, M.; Heyd, J. J.; Brothers, E.; Kudin, K. N.; Staroverov, V. N.; Kobayashi, R.; Normand, J.; Raghavachari, K.; Rendell, A.; Burant, J. C.; Iyengar, S. S.; Tomasi, J.; Cossi, M.; Rega, N.; Millam, N. J.; Klene, M.; Knox, J. E.; Cross, J. B.; Bakken, V.; Adamo, C.; Jaramillo, J.; Gomperts, R.; Stratmann, R. E.; Yazyev, O.; Austin, A. J.; Cammi, R.; Pomelli, C.; Ochterski, J. W.; Martin, R. L.; Morokuma, K.; Zakrzewski, V. G.; Voth, G. A.; Salvador, P.; Dannenberg, J. J.; Dapprich, S.; Daniels, A. D.; Farkas, Ö.; Foresman, J. B.; Ortiz, J. V.; Cioslowski, J.; Fox, D. J. *Gaussian 09*, Revision A.01; Gaussian, Inc.: Wallingford, CT, 2009.
(46) Tao, J. M.; Perdew, J. P.; Staroverov, V. N.; Scuseria, G. E. *Phys. Rev. Lett.* **2003**, *91*, 146401.
(47) Schaefer, A.; Horn, H.; Ahlrichs, R. *J. Chem. Phys.* **1992**, *97*, 2571−2577.
(48) Rega, N.; Cossi, M.; Barone, V. J. *J. Chem. Phys.* **1996**, *105*, 11060−11067.
(49) Hedegard, E. D.; Kongsted, J.; Sauer, S. P. A. *J. Chem. Theory Comput.* **2011**, *7*, 4077−4087.
(50) Tomasi, J.; Mennucci, B.; Cammi, R. *Chem. Rev.* **2005**, *105*, 2999−3093.

DOI: 10.1021/acs.inorgchem.5b01677
Inorg. Chem. 2015, 54, 9576−9587